LANGMUIR

Interface-Rich Materials and Assemblies

Functional Biointerfaces Based on Mixed Zwitterionic Self-Assembled Monolayers for Biosensing Application

Yu-Sin Wang, Shuehlin Yau, Lai-Kwan Chau, Ameen Mohamed, and Chun-Jen Huang

Langmuir, **Just Accepted Manuscript** • DOI: 10.1021/acs.langmuir.8b01779 • Publication Date (Web): 15 Aug 2018

ACS Publications

is published by the American Chemical Society. 1155 Sixteenth Street N.W., Washington, DC 20036

Functional Biointerfaces Based on Mixed Zwitterionic Self-Assembled Monolayers for Biosensing Application

Yu-Sin Wang,[†] Shuehlin Yau,[‡] Lai-Kwan Chau,[§] Ameen Mohamed,[†] Chun-Jen Huang[†,#,*]

[†] Department of Biomedical Sciences and Engineering, [#] Department of Chemical and Materials Engineering, National Central University, Jhong-Li, Taoyuan 320, Taiwan

[‡]Department of Chemistry, National Central University, Jhong-Li, Taoyuan 320, Taiwan

[§]Department of Chemistry and Biochemistry and Center for Nano Bio-Detection, National Chung Cheng University, Chiayi 621, Taiwan

*Corresponding author: cjhuang@ncu.edu.tw (C.-J.H.)

ABSTRACT

Surface modification for biosensors has focused attention for improvement of their sensitivity and specificity, particularly for the detection in complex medium. In this work, we have synthesized zwitterionic carboxybetaine- (CB-) and sulfobetaine-thiols (SB-thiols) for modification of gold substrates to form a functional self-assembled monolayer (SAM) for the immunoassay in a surface plasmon resonance (SPR) biosensor. X-ray photoelectron spectroscopy (XPS), contact angle goniometer and cyclic voltammetry were applied for characterizations of elemental composition, surface wettability and packing density, respectively. The antifouling properties of the SAMs were accessed by quantitative analysis of protein and bacterial adsorption. The results from the SAMs with single component indicated that the SB-thiol SAM provides better surface hydrophilicity, fouling resistance and packing density than the CB-thiol SAM, likely due to the ionic association of CB moieties. However, the CB-thiol with the functional carboxylate group plays a critical role in post-modification of biomolecules via commercially available amine coupling chemistry. Thus, the mixed SAMs were prepared to integrate the unique characteristics from CB- and SB-thiols to control compositions and surface properties. The immunoassay was performed in the SPR biosensor, showing that the zwitterionic mixed SAM enables immobilization of bio-recognition elements (BREs), and improved sensitivity and specificity. Consequently, the work reveals excellent and attractive versatility, antifouling and functionalizable properties of zwitterionic mixed SAM comprising of CB- and SB-thiols for biosensing applications. This surface chemistry is expected to be applicable to monitor specific molecular recognition events.

Keywords: Zwitterionic materials, antifouling coatings, self-assembled monolayers, biosensing application, thiolates

INTRODUCTION

Nonspecific adsorption occurs ubiquitously at interfaces in a daily life. Under certain circumstances, the adsorption may result in troublesome and unpleasant issues. For example, the accumulation of marine organisms on hulls can increase the hydrodynamic volume of a vessel and the hydrodynamic friction, as well as corrosion of decks.[1] Biomaterial-associated infections (BAIs) arise from active colonization of bacteria on medical devices and gradual development into biofilms, which have caused considerable medical cost, extended nosocomial stay and healthy risk.[2-34] In the same sense, nonspecific adsorption in biosensing devices occurs generally to limit their sensitivity and specificity, leading to low signal-to-noise ratio (S/N ratio).[5-7] Therefore, in addition to pursue ultrasensitive sensing transduces, tremendous efforts have been conducted for the development of functional biointerfaces to permit immobilization of bio-recognition elements and resistance of nonspecific adsorption.[6-10]

Self-assembled monolayers (SAMs) have attracted considerable attention due to their unique properties to build structures and functions on the nanometer scale. The SAMs offer precise control on the molecular level, ordered structure, high packing density, and excellent surface modification for varying physicochemical properties for a broad spectrum of applications.[11-13] The multifunctional interfaces are able to be constructed by using suitable bi-functional molecules of different terminal functional groups, which are highly desirable for development of biosensors and nanomaterials for medical uses.[14-15] Oligo(ethylene glycol) (OEG)-terminated SAMs have been developed as a stealth coating to improve biocompatibility, resist nonspecific adsorption, and good wetting property. However, to keep the colloidal stability of nanoparticles *in vivo*, OEG coatings with high molecular weight more than 2,000 Da are needed,[16-17] which adds large layer thickness. In addition, other concerns of OEG materials, such

as susceptibility to environmental conditions and ease of oxidation urge for development of alternatives.[18-23]

Inspired by natural phospholipids, zwitterions carrying both positively and negatively charged groups have been applied for harnessing nonspecific adsorption due to their characteristics of superhydrophilicity and charge balance.[15, 24-26] The strongly bound and ordered water layer at the zwitterionic interface enables to minimize the energy loss while a protein approaches.[23] Besides the bioinertness of zwitterionic coatings, Jiang's group has successfully demonstrated the functionalization capability of zwitterionic poly(carboxybetaine) (pCB) to afford conjugation of bio-active molecules while keeping the excellent antifouling properties.[7-8, 26-27] The breakthrough leads to a wide range of applications, including biosensing, in complex medium. However, the polymer-based binding platforms were developed based on a grafting from an approach, in which the initiator is firstly attached onto the surface, followed by in situ polymerization. The binding capacity and antifouling properties can be modulated by grafting density and film thicnkness.[6-7] Therefore, careful control on experimental conditions and skillful operation are required for consistent and reliable quantification of specific binding events.

In this work, we conducted a facile approach for the development of mixed zwitterionic SAMs based on carboxybetaine (CB)- and sulfobetaine (SB)-thiols for dual functionalizable and bioinert properties on a surface plasmon resonance (SPR) biosensor. The CB- and SB-thiols both carrying the propene intercharge arm between two charged groups were synthesized. The CB-thiol exhibits dual fouling resistance and functionalization under an acidic condition, in which the carboxylate group can be protonated to become the functional carboxyl group for conjugation of biomolecules via amine coupling chemistry.[6-8, 26-27] Moreover, the SB-thiol holds robust and insusceptible antifouling properties. The formation and packing density of single and mixed

SAMs were accessed and compared by using X-ray photoelectron spectroscopy (XPS), contact angle goniometer and cyclic voltammetry (CV). The antifouling properties of the mixed SAMs with different molar ratios of CB- and SB-thiols were evaluated by measuring adsorption of proteins and bacteria. Ultimately, the biosensing interface based on the mixed SAMs with conjugated bio-recognition elements was implemented for sensitive molecular detection.

EXPERIMENTAL SECTION

Materials. 11-bromo-1-undecene, dimethylamine in THF, ethyl 4-bromobutyrate, 1,3-propanesultone, anhydrous sodium acetate, sodium borate were purchased from Sigma-Aldrich. Thioacetic acid, HPLC graded methanol, anhydrous acetone, anhydrous diethyl ether, 2,2′-azobis(2-methylpropionitrile) (AIBN), hydrochloric acid (HCl), extra dry tetrahydrofuran (THF), N-hydroxysuccinimide (NHS), 1-(3-dimethylaminopropyl)-3-ethylcarbodiimide hydrochloride (EDC), HPLC graded acetonitrile, sodium hydroxide (NaOH) were supplied from ACROS Organics™. Anhydrous sodium sulfate was obtained from Alfa Aesar. Bovine serum albumin (BSA) was obtained from MDBio Inc. LIVE/DEAD® BacLight™ bacterial viability kit and peroxidase-conjugated Goat anti-Rabbit were purchased from Life Technologies. Water was purified until the resistivity value was 18 MΩ.cm using the Academic Milli-Q Water System (Millipore Corporation) and filtered using a 0.22 μm filter. Luria-Bertani broth (LB broth) was supplied from Gibco. Anti-VHL antibody rabbit polyclonal IgG was purchased from Santa Cruz Biotechnology, Inc.

Characterization Techniques. The ^{1}H NMR spectra were recorded at 600 MHz on a Bruker NMR spectrometer. The FTIR spectra were accessed using Jasco FT/IR- 410. For High-Resolution Mass spectrometry (HRMS), JEOL JMS-700 high-performance mass spectrometer was used to identify CB-thiol.

Synthesis of SB-thiol. Preparation of sulfonic acid betaine thiols followed the previous study.[25] 11-bromo-1-undecene (5 mL, 22 mmol) was dissolved in 25 mL of THF then added to 25 mL of 2 M dimethylamine solution, and the reaction mixture was stirred at 50 °C for 16 h. The solvent was removed by rotovap under reduced pressure. 200 mL of 1M NaOH was added to the concentrated product, and the organic product was collected and extracted twice from 200 mL of

diethyl ether. The organic solution was filtered through anhydrous sodium sulfate and finally concentrated by rotovap to give a clear brown oil of N,N-dimethyl-undec-10-enyl-amine with a yield of 81%.

2 g of N,N-dimethyl-undec-10-enyl-amine (10 mmol) was dissolved in 50 mL of anhydrous acetone then added 1.3 mL of 1,3-propanesultone and stirred at room temperature for 2 days. The solvent was removed under reduced pressure, and the product was dissolved by adding 2 mL of methanol. Then the solution was added dropwise to 80 mL of acetone and recrystallized. The supernatant was removed by high-speed centrifugation (9000 rpm, 5 min). Finally, vacuum drying gave a white powder of 3-(N,N-dimethyl-undec-10-enyl-amino)-propane-1-sulfonic acid with a yield of 75%.

1.5 g of 3-(N,N-dimethyl-undec-10-enyl-amino)-propane-1-sulfonic acid (4.3 mmol) was mixed with 8 mL of methanol solution which was previously bubbled with nitrogen and 2 ml of thioacetic acid in an oxygen-free atmosphere. Then 100 mg of 2,2'-azo (2-methylpropionitrile) was added to the solution, and the solution was allowed to react for 36 h in a photoreactor at a wavelength of 365 nm under an oxygen-free environment at room temperature. The solvent was removed by rotovap under reduced pressure. The resulting solution was added dropwise to 80 mL of anhydrous acetone and recrystallized. The supernatant was removed by high-speed centrifugation (9000 rpm, 5 min). Finally, vacuum drying gave a white powder with a yield of 70%.

After bubbling deionized water with nitrogen, 1 g of the product was dissolved in 10 mL of deionized water under an oxygen-free atmosphere and stirred for 5 min. Then 5 mL of 1 M aqueous solution of NaOH was slowly added at room temperature followed by stirring for 3 h.

Then 6 mL of 1 M HCl solution was added slowly. After the solvent was removed under reduced pressure, the product was dissolved in absolute ethanol and the white solid was removed by filtration. The solution was dried to give a white solid of 3-[(11-mercapto-undecyl)-N,N-dimethyl-amino]-propane-1-sulfonic acid with a yield of 82%. The total yield after 4 steps was 36%. ^{1}H NMR (D_2O, 600 MHz): δ (ppm) 1.39-1.5 (m, 14H), 1.69 (m, 2H), 1.83 (m, 2H), 2.2 (m, 2H), 2.61 (m, 2H), 3.02 (m, 2H), 3.17 (s, 6H), 3.39 (m, 2H), 3.54 (m, 2H).

Synthesis of CB-thiol. 11-bromo-1-undecene (5 mL, 22 mmol) was dissolved in 25 mL of THF then added to 25 mL of 2 M dimethylamine solution, and the reaction mixture was stirred at 50 °C for 16 h. The solvent was removed by rotovap under reduced pressure. 200 mL of 1M sodium hydroxide was added to the concentrated product, and the organic layer was collected and extracted twice from the mixed solution with 200 mL of diethyl ether. The organic solution was filtered through anhydrous sodium sulfate and finally concentrated to give a clear brown oil of N,N-dimethyl-undec-10-enyl-amine with a yield of 81%.

1.25 g of the first product (6.4 mmol) was mixed with 1.8 mL of ethyl 4-bromobutyrate (12.8 mmol) and 9 mL of acetonitrile and stirred at 50 ° C for 3 days. The solvent was removed by rotovap and the solution was added dropwise to 100 ml of diethyl ether and stirred for 10 min. The supernatant was removed, and the product was purified twice. Finally, the product was concentrated by rotovap to give dark brown oil with a yield of about 67%.

1.2 g of the second product (3 mmol) was mixed with 6 mL of methanol which was previously bubbled with nitrogen and 1.8 mL of thioacetic acid in a nitrogen atmosphere. Then 100 mg of 2,2'-azobis (2-methylpropionitrile) was added, and the mixture was allowed to react in a photoreactor at a wavelength of 365 nm for 36 h in the nitrogen environment at room

temperature. The solvent was removed by rotovap under reduced pressure. The solution was added dropwise to 100 mL of diethyl ether for 10 min with stirring. The supernatant was removed, and the product was purified twice. Finally, the product was concentrated by rotovap to obtain yellow oil with a yield of about 70%.

After bubbling deionized water with nitrogen, 1.05 g of the third product was dissolved in 10 mL of deionized water under nitrogen atmosphere and stirred for 5 min. Then 5 mL of 1 M aqueous sodium hydroxide was slowly added at room temperature followed by stirring for 3 h. Then 6 mL of 1 M HCl solution was added slowly. The solvent was removed by rotovap under reduced pressure. The product was dissolved in absolute ethanol and filtered to remove the white solid. The solution was then added dropwise to 150 mL of diethyl ether with stirring for 10 min, and the supernatant was removed. After the final product of CB-thiol was concentrated by rotovap, bright yellow oil was obtained with a yield of about 75%. The total yield after 4 steps was 26%. The FTIR, HRMS and ^{1}H NMR spectra supported the structure of CB-thiol. IR (cm^{-1}): 1727 (C=O, COOH), 1645 (COO^-) and 1485 ($-N^+(CH_3)_2-$). ^{1}H NMR (D_2O, 600 MHz): δ (ppm) 1.213-1.309 (m, 14H), 1.632 (m, 2H), 1.792 (m, 2H), 2.067 (m, 2H), 2.55 (m, 2H), 3.158 (m, 4H), 3.343 (s, 6H), 3.369 (m, 2H). HRMS-FAB: m/z 318.5 ($[M + H]^+$; calcd for $C_{16}H_{35}NO_3SH$, 318.25). The synthesis procedures for SB-thiol and CB-thiol are summarized in Scheme 1.

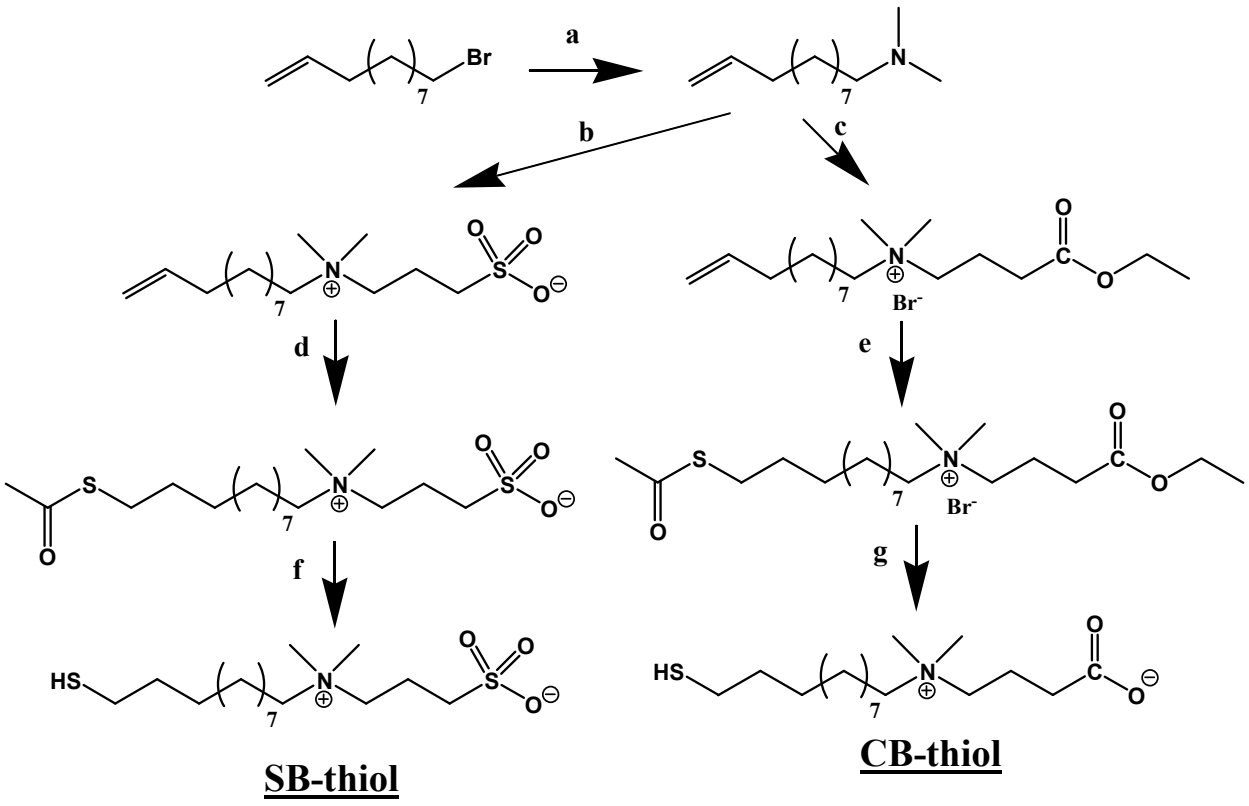

*a) dimethylamine, THF, 50 ° C, 16 h; b) 1,3-Propanesulfone, acetone, RT, 24 h; c) ethyl 4-bromobutyrate, acetonitrile, 50 ° C, 3 days; d) and e) thioacetic acid, AIBN, CH_3OH, hv, RT, 16 h; f) and g) NaOH, RT, 3 h.

Scheme 1. Sythesis of SB-thiol and CB-thiol.*

Preparation of SAM. The glass substrate was cleaned with O_2 plasma before coating then a gold film (thickness = 48 nm) was deposited on a glass slide coated with an adhesion promoting chromium film (thickness = 2 nm) by an E-Gun & Thermal to prepare a gold chip. For the single SAM preparation on a gold substrate, the CB- and SB-thiol SAMs were prepared individually in PBS solution at the concentration of 2 mM. For the mixed SAM prepared on the gold substrate, the molar ratios of CB-thiol to SB-thiol in PBS solutions were 0, 0.1, 0.3, 0.5, 0.7,

0.9 and 1 while the total concentration of all the solutions was 2 mM. The coating time and temperature for all the solutions were 25^{o}C and 20 h, respectively. After coating the substrate, it was washed with ethanol and dried in a stream of nitrogen.

Contact Angle Measurements. Water static contact angle measurements were performed by a contact angle goniometer (Phoenix mini, Surface Electro Optics, Seoul) equipped with Surfaceware9 software and a CCD camera for imaging acquisition and analysis. The measurement was performed at least four times at random positions. The microsyringe produces 5μL water droplets and the droplets were placed on samples for the contact angle measurements. The pH-dependent measurements for the CB-thiol and SB-thiol SAMs were performed using water solutions at different pH values ranging from 4 to 10. Since the ions in buffers can tune a range of properties of charged polymers at the solid/liquid interface such as hydration, conformation, stiffness, surface wettability, lubricity, and adhesion,[28-29] the ion effect was excluded by using water for the pH-dependent contact angle measurements.

XPS Analysis. Surface elemental analysis and chemical composition identification was carried out using XPS equipped with microfocused and monochromatic Al Kα X-ray source (25 W, 1486.6 eV; Sigma Probe, Thermo Scientific). The takeoff angle of the photoelectron (with respect to the surface) was set at 45°. A dual beam charge neutralizer (7 V Ar^{+} and flooding 3 kV, 1 μA electron beam) was used to compensate the surface charging effects. The vacuum level of the system was set below 10^{-6} Pa using anoil-less ultrahigh vacuum pumping system. The spectra were obtained with a pass energy of 58.7 eV while the binding energy measured was calibrated against the Au $4f_{7/2}$ peak at 84 eV.

Bacterial Adsorption Test. *E.coli* and *S.epidermidis* were collected from a single bacterial colony and cultured in a conical flask contained 5 mL LB for overnight at 37 ^{o}C. Then the

bacteria were washed with sterile PBS solution by centrifugation at 4000 rpm for 5 min and re-suspend thrice in PBS solution. For testing the antifouling properties of the substrates, a bacterial solution with an optical density reading at 670 nm (OD670) of 0.1 (~8×10^7 cells/mL) was obtained by diluting the bacterial samples with PBS. The substrates were immersed into the bacterial solution at 37 °C for 3 h, followed by washing with sterile PBS and agitating at 100 rpm for 5 min for three times to remove loosely-adherent bacteria. The adsorbed bacteria were then prepared for fluorescence microscopy by staining with 30 µL of LIVE BacLight for 15 min. After the substrates were rinsed with PBS in a shaker at 100 rpm for 5 min, the green light emitted from living bacteria with the integrated intensity of the spectrum between 510–540 nm was inspected under a fluorescence microscopy (Zeiss Microscope Axio Observer A1, Germany) with a magnification of 200x and an excitation wavelength of 488 nm. The numbers of bacteria were analyzed using an ImageJ software package (developed at National Institutes of Health, MA).

SPR measurement. The SPR sensor used was developed at the Institute of Photonics and Electronics, Prague, Czech Republic and the refractive index change was detected by a commercial refractometer DSR-lambda (Schmidt Haensch GmbH, German). First, the sensor response was calibrated using PBS, introduced at a flow rate of 18 µL/min. The flow rate was kept constant for all the injected solutions, and the temperature was set at 25 ± 0.01 ° C. Then, 0.3 % NaCl was added to the running buffer for 10 min through the flow-cell, and the change in the sensor response was detected by the refractometer to establish a calibration factor.[30-31] BSA solution at a concentration of 1 mg/mL was injected for 15 min while the surface concentration of BSA was estimated based on the equivalent change of the refractive index. It was previously reported that the sensor response is expressed in the equivalent of refractive index change

expressed in 10^{-3} RIU (mRIU) and the addition of 0.3% NaCl increased the refractive index of the running buffer by 4.68×10^{-4} refractive index units (RIU).[30-31] When the surface density of BSA was 1 ng/cm^2, the equivalent refractive index change was about 0.01 mRIU. Using all the previous relations, the adsorption level (the mass of BSA adsorbed per cm^2) on the surface was calculated.[32]

Electrochemical Analysis. Cyclic voltammetry (CV) measurements were recorded using potentiostat CHI 627 installed with CHI614A Electrochemical Analyzer software. The electrochemical cell was composed of a platinum counter electrode, Ag/AgCl reference electrode, and SAM-modified Au (111) served as a working electrode. The Au (111) working electrode was prepared as previously described.[33] The cyclic voltammograms were recorded at a scan rate of 50 mV/s in 0.1 M KCl as an electrolyte solution containing aqueous 1 mM ($K_3Fe(CN)_6/K_4Fe(CN)_6$) as an electrochemical probe.

Molecular Detection. For the measurement of biorecognition events, the mixed SAM surfaces at a molar ratio of CB-thiol of 0.1 were functionalized with either chicken polyclonal anti-BSA antibody or rabbit Anti-VHL antibody, and the functionalization procedures were monitored with the SPR sensor. The mixed SAM-coated sensor chip was mounted on the SPR sensor. To activate the carboxylate groups of the mixed SAM surface, a freshly prepared solution of NHS (0.05 M) and EDC (0.2 M) in MilliQ water was introduced for 15 min at 25 °C and the flow rate was set at 18 μL/min. Then a 10 mM sodium acetate buffer (SAb) at pH 5.5 was injected to obtain a stable baseline. The antibody solutions with a concentration of 50 μg/mL in 10mM sodium borate buffer (SBb) with pH 8.5 were flowed over the activated mixed SAM surface for 15 min. The functionalized surface, then, was washed to remove all non-covalently bound ligands using 10 mM phosphate buffer (pH 8.2) and 0.3 M NaCl solution, (PBNa). The

residual NHS esters were also hydrolyzed back to carboxylate anions in the phosphate buffer, and, accordingly, the surface was completely deactivated to determine the number of immobilized antibodies. The surface density of immobilized antibodies on mixed SAM surfaces was in the range of 40-50 ng/cm^2. For the measurements of molecular detection, the solutions containing the target molecules, Goat anti-Rabbit secondary IgG, at a concentration of 8, 80, 800 and 8000 ng/mL were allowed to flow through the functionalized mixed SAM surfaces for 15 min at room temperature at a flow rate of 18 μL/min. The total adsorption level was determined as the difference in the sensor response between the PBS buffer baselines (before the sample injection) and after washing the reacted surface for 15 min.

RESULTS and DISCUSSION

Characterization of single SAMs on gold. Gold substrates were modified with a single SAM of either SB-thiol or CB-thiol. The interfacial elemental and composition analysis for the SAMs was performed using XPS. In Figure 1a, the spectra exhibiting spin orbital split doublet are centered at binding energies (BEs) of 167.0 and 168.2 eV, which are referred to the sulfonate (-$\underline{S}O_3^-$) group in SB-thiol.[34-35] The other two unresolved components centered at BEs of 161.9 and 163.1 eV binding energies correspond to the $S2p_{3/2}$ and $S2p_{1/2}$ of Au-$\underline{S}$, respectively.[36] For the S2p spectrum of the CB-thiol SAM in Figure 1b, a doublet structures for Au-$\underline{S}$ appear along, consistent with the sulfur atoms bound to the gold surface as a thiolate species.[36] Additionally, the N1s spectra for SB- and CB-thiol SAMs in Figure 1c show peaks with a BE of 402.5 eV due to the presence of the quaternary ammonium moiety.[34-35, 37-38] Table 1 shows the elemental concentrations of SAMs on gold as determined by XPS. The atomic molar ratio of N/S is 1.09 for the CB-thiol SAM, which is consistent approximately to the theoretical value. Similarly, for SB-thiol, the experimental atomic molar ratio of N/S is 0.48, close to the calculated theoretical value of 0.5. Collectively, evidences from XPS measurements support that SB- and CB-thiol molecules were assembled on gold. However, the formation and packing density of SAMs in addition to the surface chemistry strikingly influence their performance, which are needed to be further investigated.

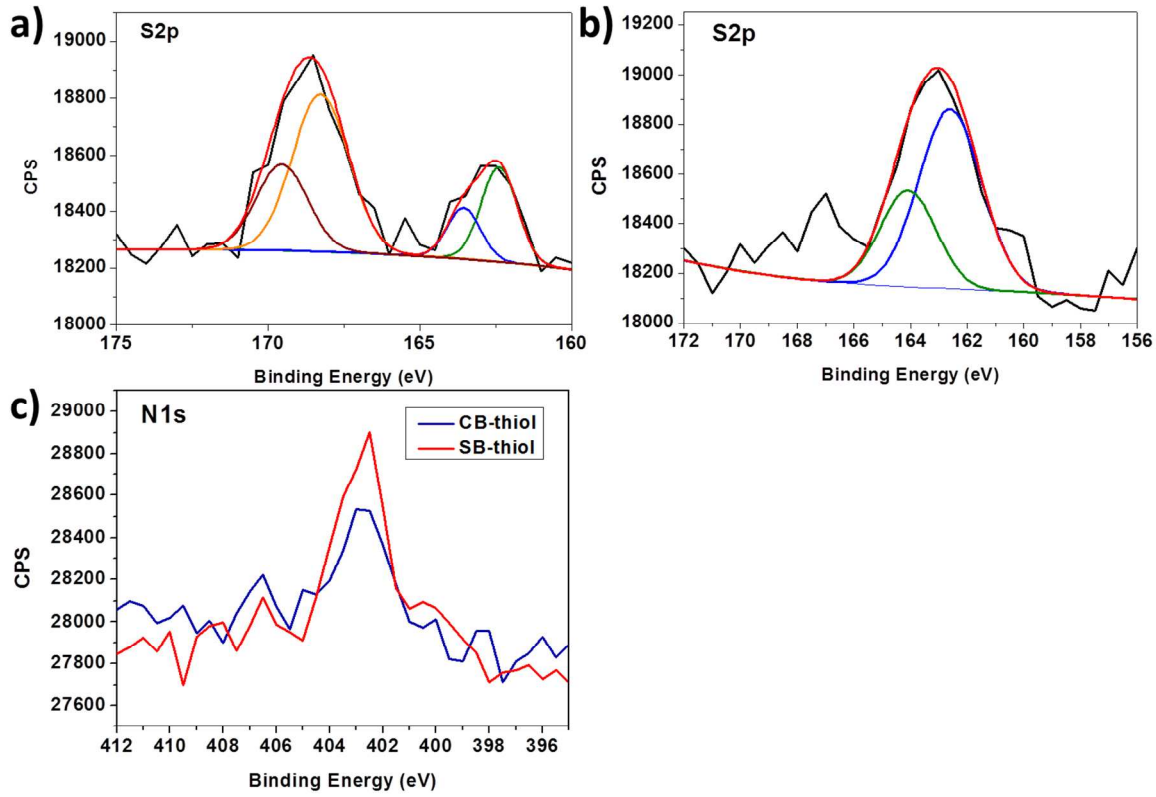

Figure 1. XPS spectra for S2p (black lines) acquired from the SB-thiol SAM (a), and CB-thiol SAM (b). XPS spectra for N1s acquired from SB- (red line) and CB-thiol (blue line) SAMs (c).

Table 1. Elemental Composition of SAMs on Gold As Determined by XPS

Atom		C	N	O	S	N/S Calculated	N/S Experimental
Atomic percentage (%)	CB-thiol SAM	32.36	1.1	28.49	1.01	1	1.09
	SB-thiol SAM	55.27	1.87	22.73	3.9	0.5	0.48

Protonation of zwitterionic molecules can be affected by the pH value of a solution and may lead to structural disorder and loss of charge balance. Therefore, the surface wetting properties of the SAMs associated with the pH values of water solutions were investigated by water contact angle measurements. As shown in Figure 2, the superhydrophilicity of SB-thiol SAMs was insusceptible to the pH changes, and the contact angles were around 5°. On the other hand, the contact angles of the CB-thiol SAMs in the measured pH range show a noticeable transition from 16.7° to 39.5° between pH 5-6. Herein, the SB group remains the strong hydration over a wide pH range, which is attributable to the characteristic of zwitterionic property and low pK_a to allow fully charged in a solution with low pH value. The difference in the wetting behavior between CB- and SB-thiol SAMs was found in the silane systems,[39] where the CB-silane film exhibits superhydrophilic; the SB-silane film is total wetting.

From the data reported previously from CB-based surfactants, the pK_a values vary upon the carbon number in the intercharge arm from 1.8 to 5.12 in water at room temperature.[40-41] Interestingly, for the CB-thiol SAMs, the surface becomes hydrophobic at a pH value above the pK_a, which is supposed to be the fully ionized state. This should be due to the occurrence of inter- and intra-molecular ion-pairing events, giving rise to the hindrance of charged groups and exposure of alkane domains (Scheme 2).[23, 42-43] The ionic association depends strongly on the configuration of an ionic group, solvent, and ionic strength. The intramolecular pairing requires the bending around the headgroup to ionically bridge the inner charge or neutralization of the charges through space to form a ring-type structure. Additionally, a decrease in pK_a may indicate a stronger associative interaction between ammonium and carboxylate.[23 41, 44] It is also suspected that the self-assembled structure of CB-thiol on gold allows the intermolecular ion-pairing due to the short molecular distance.[45] Therefore, in this work, the high contact angle for the CB-thiol

SAMs when the pH above the pK_a should be contributable to the ionic association. In addition, the carboxylic acid (COOH) terminated SAMs, such as the CB-thiol SAM at low pH, exhibit interfacial hydrogen bonding, which can influence surface wetting, molecular structure and double-layer potential.[46-48] In the process for the activation and functionalization of carboxylic acid groups, the hydrogen bonding should be considered for effective and optimized conjugation.[8]

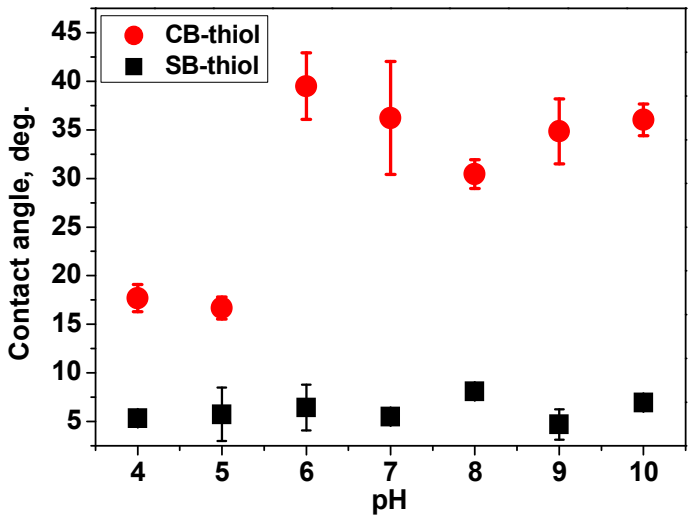

Figure 2. Static water contact angle measurement of SB- and CB-thiol SAMs as a function of pH.

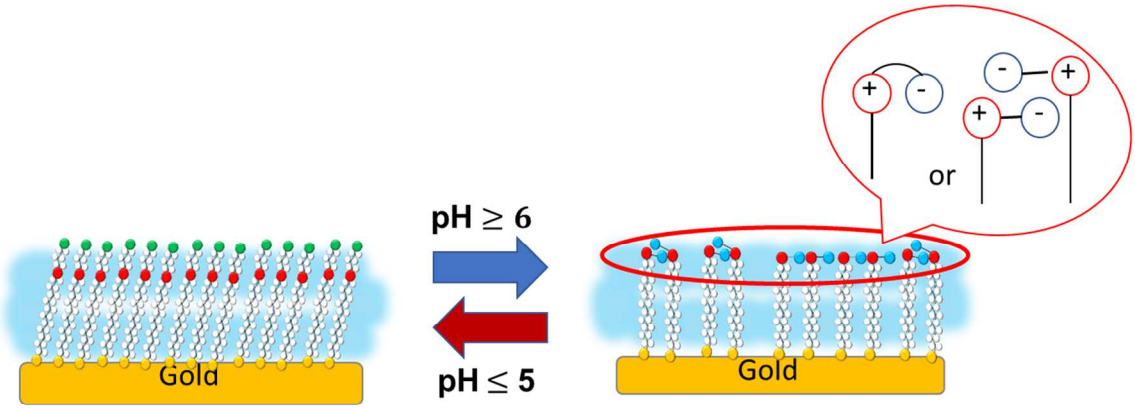

Scheme 2. Inter- and intra-molecular ion-pairing events modulated by pH values.

To examine the packing density and integrity of the monolayers on the gold surface, cyclic voltammetry was used to analyze the SAM modified gold electrodes in the presence of $Fe(CN)6^{3-/4-}$ as a redox probe.[49-50] The electrochemical experiments were conducted in 0.1 M KCl solution containing 1mM redox couple $Fe(CN)_6^{3-/4-}$at a scan speed of 0.1 V/s in a sweep range from -0.2 to 0.8 V. In Figure 3, well-defined characteristic redox waves of the couple can be observed on the bare Au electrode. After deposition of CB- and SB-thiols on gold substrates, the anodic and cathodic current at a gold electrode decreased. The peak current decreased more significantly with the SB-thiol SAM compared to that obtained at the bare electrode and CB-thiol SAM. Moreover, when the SB-thiol SAM is adsorbed on the gold electrode, we observe an experimental wave with a much larger overpotential (i.e., anodic and cathodic peak potentials are spaced by 273 mV) than those of bare gold and CB-thiol deposited electrodes, which are 76 and 64 mV, respectively. The electron transfer at an electrode can occur by three possible ways: (1) a tunneling process; (2) permeation of the redox species into the adlayer; and (3) diffusion of the

electroactive compound inside pinhole or defect sites of the limited exposed electrode surface. It has been found that the decrease of the peak currents and large overpotential can be associated with slow diffusion through a pinhole and/or permeation into the monolayers.[51] Therefore, the SB-thiol SAM served as the electron-transfer barrier to hinder the tunneling of electrons due to increased thickness and dense structure of the adlayer.[49-50] On the contrary, the CB-thiol SAM displayed less capability to block the electron transfer, which may reflect the high contact angles in Figure 2.

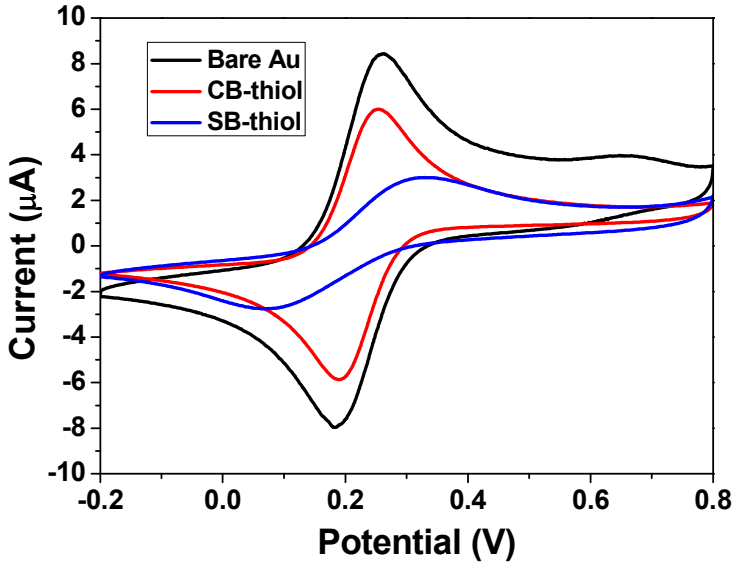

Figure 3. Cyclic voltammograms of SAMs on gold electrode. Redox reactions of bare gold (black), CB-thiol SAM (red) and SB-thiol SAM (blue) were measured.

The SPR biosensor was employed to quantify the antifouling properties of SAMs. The SAMs from CB- and SB-thiols were prepared in PBS as a good solvent for optimized packing density and conformation.[52] After the baseline was established, BSA solution with a

concentration of 1 mg/mL was flow over the samples in the SPR sensor, followed by washing with PBS. The time-resolved sensorgrams are shown in Figure 4, in which the signal change for bare gold was significantly higher than that for modified substrates. Additionally, the SB-thiol SAM provided better antifouling properties than that of the CB-thiol SAM. The protein adsorption levels after washing with PBS on different substrates were estimated according to previous literature,[28-29, 48] indicating 102.7 ± 4.1, 36.8 ± 5.9 and 0.03 ± 0.04 ng/cm^2 for bare gold, CB- and SB-thiol SAMs respectively.[30-31, 53] Obviously, the SB-thiol SAM can effectively repel BSA from the surface to the ultralow fouling level.[54] The results from the SPR sensor reflect the findings from the contact angle and CV measurements, where the CB-thiol SAM exhibits less hydrophilicity and packing density than the SB-thiol SMA. Herein, in order to develop a suitable biointerface for biosensing, the functional group and antifouling background are demanded for bio-recognition element (BRE) conjugation and resistance against non-specific adsorption. In this sense, the combination of CB- and SB-thiols for development of the biointerface may offer an opportunity to integrate the unique characteristics of both thiols together in the biosensing application.

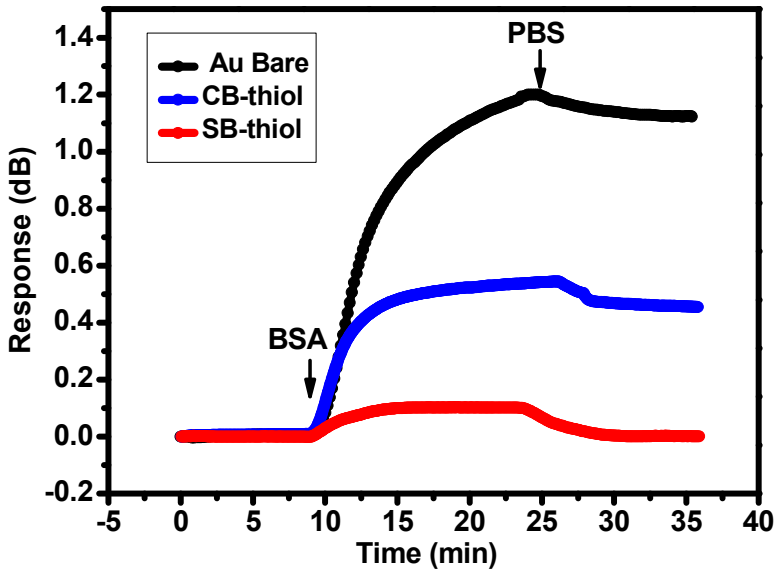

Figure 4. SPR sensorgrams for protein adsorption on bare gold, CB- and SB-thiol modified substrates. The SAMs were prepared in PBS.

The surface composition of mixed SAMs was correlated with complex interactions among thiol molecules, substrate and solvent.[55] In this study, the mixed SAMs were formed in CB- and SB-thiol solutions with different mole fractions in PBS. The surface elemental composition and wetting property of the mixed SAMs were characterized using XPS and contact angle measurements, respectively. In XPS measurements, the elemental ratio of $S_{sulfonate}/N_{ammonium}$ was obtained by analyzing the corresponding components of sulfonate and quaternary ammonium groups in XPS spectra of S2p and N1s. In Figure 5a, the $S_{sulfonate}/N_{ammonium}$ ratios proportionally decreased with increase in the CB-thiol mole fractions in the solutions. Moreover, in Figure 5b, the water contact angles on mixed SAMs increased with the mole fraction of CB-thiols in the sample preparation process. It was indicated that more CB-

thiol in the surface composition the higher degree of hydrophobicity. Therefore, from the surface elemental analysis and contact angle measurements, the surface composition of the SAMs as well as the interfacial phenomena can be readily controlled by varying the thiol molar ratio in the preparation solution. The versatility of the SAM technology has been proven to be very attractive to precisely modulate surface properties for various applications. In this work, we provide the first evidence to accomplish the mixed zwitterionic SAMs with fine control over the molecular composition.

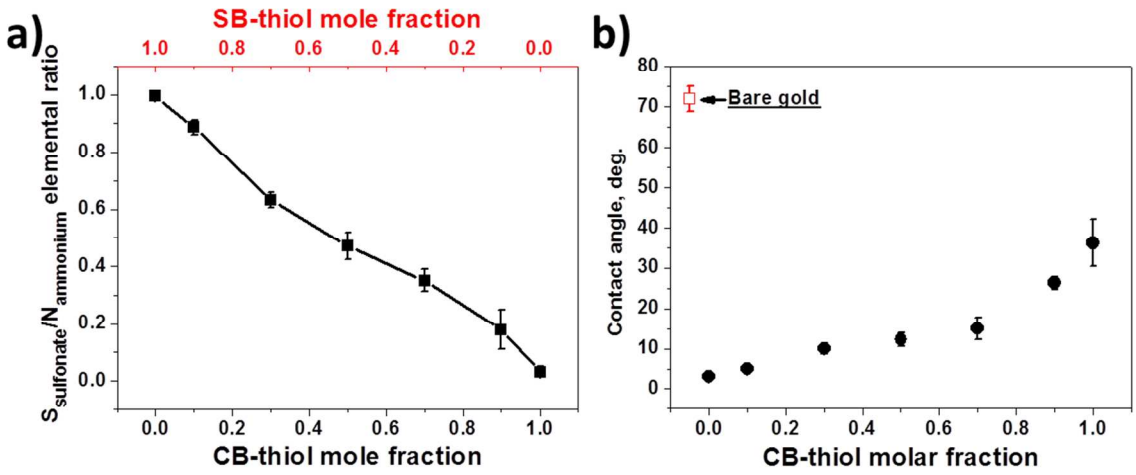

Figure 5. The $S_{sulfonate}/N_{ammonium}$ elemental ratio as a function of thiol mole fraction in PBS (a). Water contact angle as a function of CB-thiol molar fraction in PBS (b). The red hollow square indicates the contact angle for bare gold.

To examine the antifouling properties of the mixed SAMs, tests for the bacterial and protein adsorption were carried out on SAMs with different compositions. For bacterial adsorption, substrates were immersed in the bacterial solutions of Gram-negative *E. coli* and Gram-positive *S. epidermidis* and then the presence of the bacteria on surfaces was verified by staining with the LIVE/DEAD dye. The fluorescence images of the adsorbed bacteria were taken and quantitatively analyzed by ImageJ software as found in Figure 6. It appears that the adsorption levels for both bacteria decrease with the CB-thiol mole fractions and bacteria of *E. coli* exhibit stronger adhesion onto the SAMs than *S. epidermidis*. Among the samples, the pure SB-thiol SAM and mixed SAM with a CB-thiol mole fraction of 0.1 display considerable reduction in bacterial adsorption by more than 99% with respect to bare substrates.

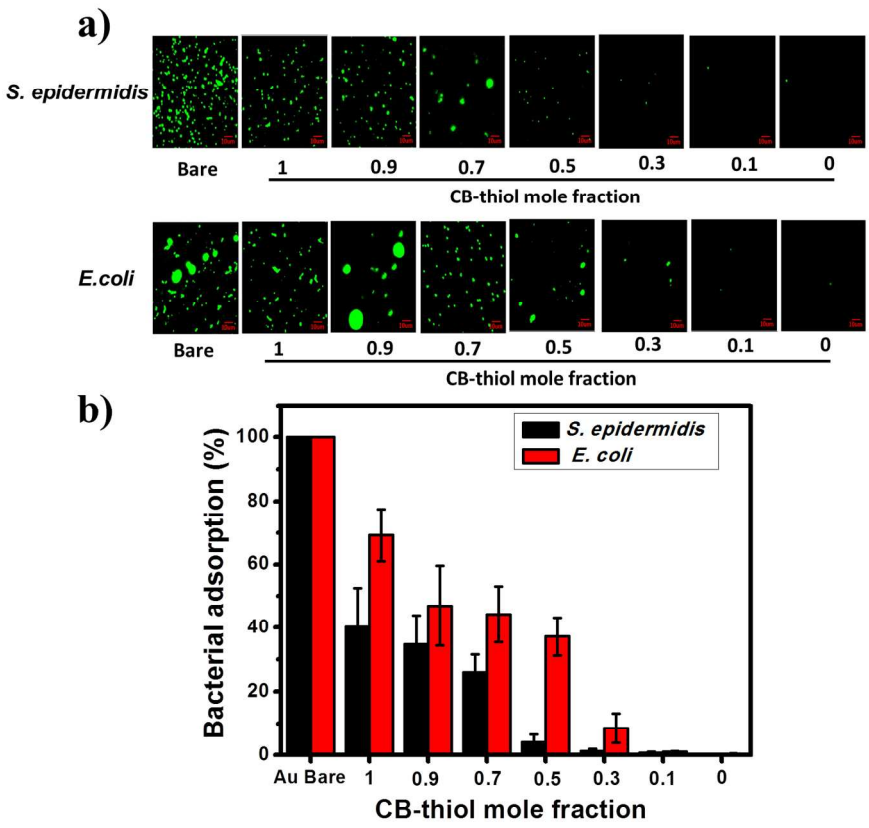

Figure 6. (a) Fluorescent images of adsorbed *S. epidermidis* and *E. coli* on bare gold and mixed SAM modified substrates. The scale bars in all images are 10 μm. (b) The quantitative data for the adsorbed bacterial numbers on bare gold and mixed SAM modified substrates.

For the SPR measurements, non-specific protein adsorption on the mixed SAMs was quantitatively evaluated by contacting BSA at a concentration of 1mg/mL, followed by washing with PBS. The SAMs prepared on gold substrates from different CB-thiol mole fractions with respect to the total mole number of thiols. The time-resolved SPR sensorgrams were recorded in Figure 7a. The adsorption levels of BSA were well correlated to the mole fractions as found in bacterial adsorption. When the mole fraction of CB-thiol in the SAMs decreased, the fouling resistance against protein adsorption increased, showing the excellent antifouling properties of SB-thiols. The amount of the adsorbed protein was evaluated from the sensorgrams as shown in Figure 7b. The fouling level of the mixed SAM with the CB-thiol mole fraction of 0.1 was as low as 5.5 ± 1.8 ng/cm^2, corresponding to the reduction of 95% of the non-specific protein adsorption compared with that on a bare gold substrate. Taken results from the bacterial and protein adsorption, SB-thiol in mixed SAMs enables to repel the non-specific adsorption effectively to avoid the false positive signal for the biosensing purpose. CB-thiol can provide the functional group for conjugation of BREs, and thus the combination of CB- and SB-thiol in mixed SAMs will lead to an appropriate binding platform on biosensors.

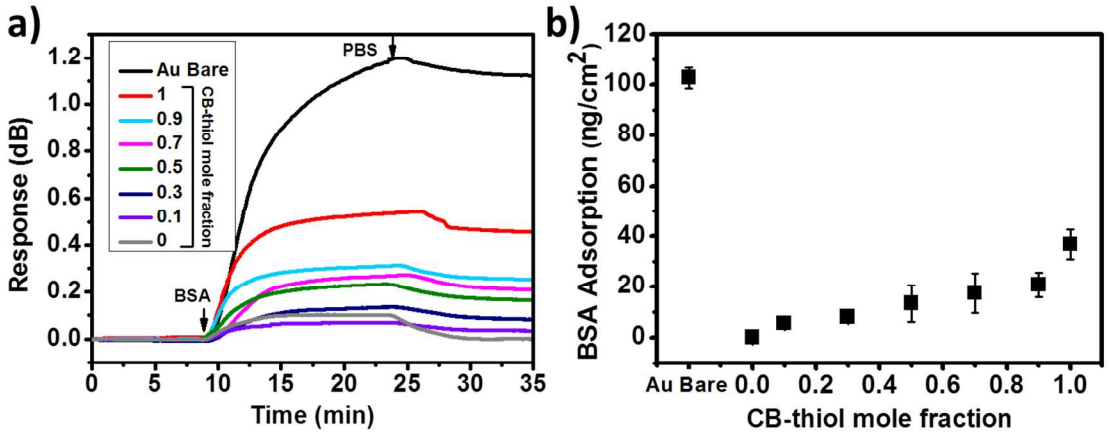

Figure 7. (a) SPR time-resolved sensorgrams for protein adsorption results on mixed SAM with CB-thiol mole fractions of 0, 0.1, 0.3, 0.5, 0.7, 0.9 and 1. (b) The quantitative data for protein adsorption levels.

The zwitterionic mixed SAM with a CB-thiol mole fraction of 0.1 was employed for molecular detection on a SPR biosensor. In this work, the detection was performed based on recognition interaction between primary and secondary antibodies. Primary rabbit antibody as a target molecule and chicken antibody as a nontarget molecule were individually immobilized on the mixed SAMs via the EDC/NHS amine coupling chemistry. In Figure 8, the SPR sensorgram shows the functionalization process and the response difference after attachment of antibodies. The amount of immobilized primary antibodies on the surface was estimated to be 45.5 ± 5.4 ng/cm^2, which is comparable to the previous work.[27] The result proved that the zwitterionic mixed SAMs afford post-functionalization and protein conjugation for ready application in biosensing.

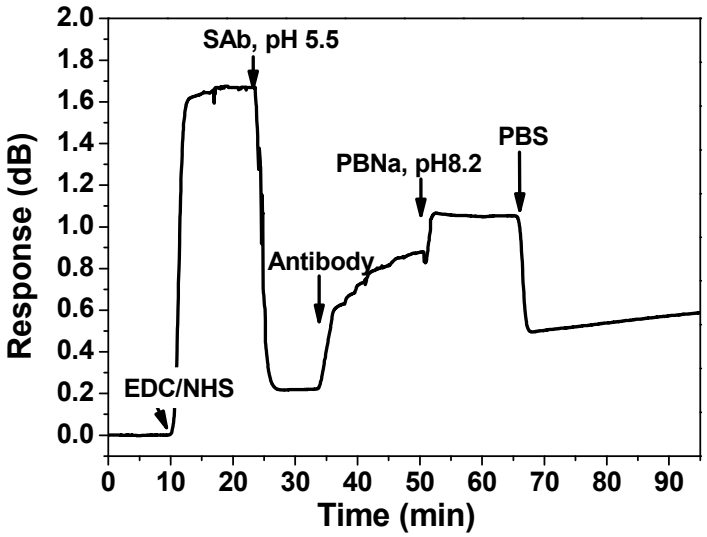

Figure 8. SPR sensorgram for antibody conjugation on mixed SAMs using EDC/NHS coupling chemistry.

To compare the specific recognition and antifouling properties of the functional zwitterionic mixed SAMs on SPR, the molecular detections of target (rabbit polyclonal IgG) and nontarget (chicken polyclonal IgG) primary antibodies immobilized on SPR chips were acommplished by individually flowing solutions containing secondary goat anti-rabbit antibodies at concentrations ranging from 8 ng/mL to 8 μg/mL. The SPR sensorgrams are present in Figure 9a, revealing that on the chips modified with the target primary antibodies the responses increased with the concentrations of secondary antibodies. On the contrary, the responses to the interaction between the analytes and immobilized nontarget molecules were relatively small after washing with the buffer. The calibration curves and the limit of detection (LOD) were shown in Figure 9b. The LOD of 55.8 ng/mL was determined for which the B-Spline fit of calibration

curve reaches 3-fold standard deviation of the baseline SPR signal. The low LOD is in the same order as the detection limit of the ELISA kit and nanobead enhanced assay.[56] Moreover, the responses from the nontarget experiments are lower than the baseline noise, indicating the high specificity of the detection due to the effective repulsion of non-specific adsorption and high recognition interaction of antibody pairing. Therefore, the label-free and sensitive detection on the functional biointerface of zwitterionic mixed SAMs was demonstrated in the immunoassay. The signal-to-noise ratio of the sensor was further enhanced by the optimized surface chemistry. Consequently, the antifouling, functionalizable and versatile zwitterionic mixed SAM with precisely controlled composition and architecture holds great promise in biosensing and other specific applications where the specific recognition events occur.

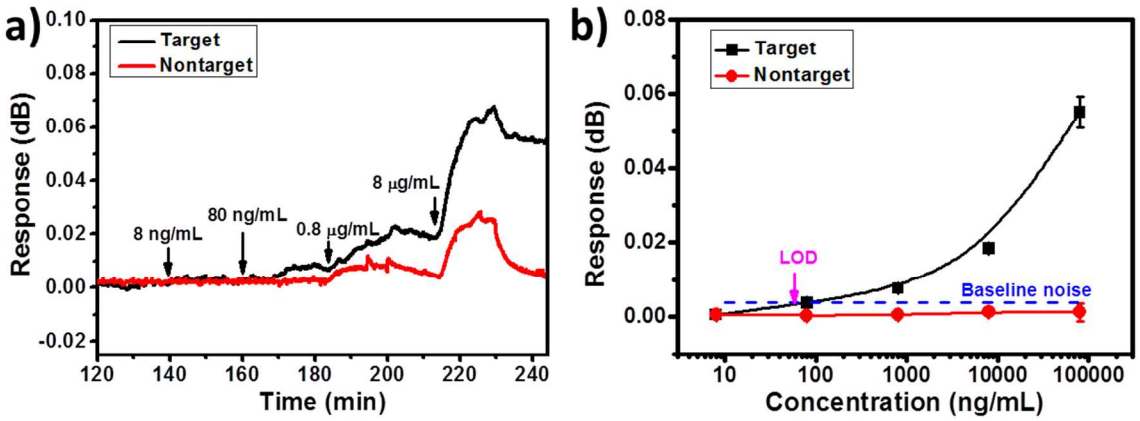

Figure 9. (a) SPR sensorgrams for the detection of target (rabbit polyclonal IgG) and nontarget (chicken polyclonal IgG) primary antibodies on mixed SAMs by flowing secondary antibodies (goat anti-rabbit IgG) at concentrations from 8 ng/mL to 8 μg/mL. (b) Calibration curve of SPR

biosensor for detection of target (squares) and nontarget (circles) secondary antibodies fitted with a B-Spline function. The baseline noise and LOD are indicated.

CONCLUSIONS

It is shown that zwitterionic mixed SAMs comprising of CB- and SB-thiols can be used to control compositions, antifouling, and functionalizable properties, which were successfully developed for sensitive and specific molecular detection on a SPR biosensor. By comparing with single-component SAMs made of CB-thiol, SB-thiol SAM was packed more densely and exhibited better fouling resistance. Moreover, CB-thiol offered the functionalizable feature, allowing post-modification of biomolecules via commercially available EDC/NHS amine coupling chemistry. The combination of CB- and SB-thiols in a SAM led to great versatility to finely tune interfacial properties. In this work, the real-time immunoassay was performed on the zwitterionic mixed SAM in an optical SPR biosensor, showing that the sensitivity and specificity of detection were accomplished to meet the critical requirements for medical applications. Ultimately, the surface modification via tethered CB- and SB-thiols offers a substantial potential in developing functional interfaces, and can be applied to a wide range of applications.

ACKNOWLEDGMENT

The authors acknowledge the Ministry of Science and Technology (MOST 105-2628-E-008 -007 -MY3; MOST 106-2119-M-194 -002) for financial support of this project.

REFERENCES

1. Baier, R. E., Surface behaviour of biomaterials: The theta surface for biocompatibility. *J. Mater. Sci.-Mater. Med.* **2006,** *17* (11), 1057-1062.
2. Hall-Stoodley, L.; Costerton, J. W.; Stoodley, P., Bacterial biofilms: from the natural environment to infectious diseases. *Nat. Rev. Microbiol.* **2004,** *2* (2), 95-108.
3. Stewart, P. S.; Costerton, J. W., Antibiotic resistance of bacteria in biofilms. *Lancet* **2001,** *358* (9276), 135-138.
4. Maki, D. G.; Kluger, D. M.; Crnich, C. J., The risk of bloodstream infection in adults with different intravascular devices: A systematic review of 200 published prospective studies. *Mayo Clin. Proc.* **2006,** *81* (9), 1159-1171.
5. Johnson, B. N.; Mutharasan, R., Reduction of nonspecific protein adsorption on cantilever biosensors caused by transverse resonant mode vibration. *Analyst* **2014,** *139* (5), 1112-1120.
6. Huang, C. J.; Brault, N. D.; Li, Y. T.; Yu, Q. M.; Jiang, S. Y., Controlled hierarchical architecture in surface-initiated zwitterionic polymer brushes with structurally regulated functionalities. *Advanced Materials* **2012,** *24* (14), 1834-1837.
7. Huang, C. J.; Li, Y. T.; Jiang, S. Y., Zwitterionic polymer-based platform with two-layer architecture for ultra low fouling and high protein loading. *Analytical Chemistry* **2012,** *84* (7), 3440-3445.
8. Vaisocherová, H.; Yang, W.; Zhang, Z.; Cao, Z.; Cheng, G.; Piliarik, M.; Homola, J.; Jiang, S., Ultralow fouling and functionalizable surface chemistry based on a zwitterionic polymer enabling sensitive and specific protein detection in undiluted blood plasma. *Analytical Chemistry* **2008,** *80* (20), 7894-7901.
9. Lofas, S.; Johnsson, B., A novel hydrogel matrix on gold surfaces in surface-plasmon resonance sensors for fast and efficient covalent immobolization of ligands. *J. Chem. Soc.-Chem. Commun.* **1990,** (21), 1526-1528.
10. Banerjee, I.; Pangule, R. C.; Kane, R. S., Antifouling coatings: recent developments in the design of surfaces that prevent fouling by proteins, bacteria, and marine organisms. *Advanced Materials* **2011,** *23* (6), 690-718.
11. Love, J. C.; Estroff, L. A.; Kriebel, J. K.; Nuzzo, R. G.; Whitesides, G. M., Self-assembled monolayers of thiolates on metals as a form of nanotechnology. *Chemical Reviews* **2005,** *105* (4), 1103-1169.
12. Nuzzo, R. G.; Dubois, L. H.; Allara, D. L., Fundamental-studies of microscopic wetting on organic-surfaces. 1. Formation and structural characterization of a self-consistent series of polyfunctional organic monolayers. *Journal of the American Chemical Society* **1990,** *112* (2), 558-569.

13. Kondoh, H.; Kodama, C.; Nozoye, H., Structure-dependent change of desorption species from n-alkanethiol monolayers adsorbed on Au(111): Desorption of thiolate radicals from low-density structures. *J. Phys. Chem. B* **1998,** *102* (13), 2310-2312.
14. Chaki, N. K.; Vijayamohanan, K., Self-assembled monolayers as a tunable platform for biosensor applications. *Biosens. Bioelectron.* **2002,** *17* (1-2), 1-12.
15. Garcia, K. P.; Zarschler, K.; Barbaro, L.; Barreto, J. A.; O'Malley, W.; Spiccia, L.; Stephan, H.; Graham, B., Zwitterionic-coated "stealth" nanoparticles for biomedical applications: recent advances in countering biomolecular corona formation and uptake by the mononuclear phagocyte system. *Small* **2014,** *10* (13), 2516-2529.
16. Choi, H. S.; Ipe, B. I.; Misra, P.; Lee, J. H.; Bawendi, M. G.; Frangioni, J. V., Tissue- and organ-selective biodistribution of NIR fluorescent quantum dots. *Nano Lett.* **2009,** *9* (6), 2354-2359.
17. Daou, T. J.; Li, L.; Reiss, P.; Josserand, V.; Texier, I., Effect of poly(ethylene glycol) length on the in vivo behavior of coated quantum dots. *Langmuir* **2009,** *25* (5), 3040-3044.
18. Han, S.; Kim, C.; Kwon, D., Thermal-degradation of poly(ethylene glycol). *Polym. Degrad. Stabil.* **1995,** *47* (2), 203-208.
19. Han, S.; Kim, C.; Kwon, D., Thermal/oxidative degradation and stabilization of polyethylene glycol. *Polymer* **1997,** *38* (2), 317-323.
20. Li, L. Y.; Chen, S. F.; Jiang, S. Y., Protein interactions with oligo(ethylene glycol) (OEG) self-assembled monolayers: OEG stability, surface packing density and protein adsorption. *J. Biomater. Sci.-Polym. Ed.* **2007,** *18* (11), 1415-1427.
21. Choi, H. S.; Liu, W.; Misra, P.; Tanaka, E.; Zimmer, J. P.; Ipe, B. I.; Bawendi, M. G.; Frangioni, J. V., Renal clearance of quantum dots. *Nat. Biotechnol.* **2007,** *25* (10), 1165-1170.
22. Estephan, Z. G.; Schlenoff, P. S.; Schlenoff, J. B., Zwitteration As an Alternative to PEGylation. *Langmuir* **2011,** *27* (11), 6794-6800.
23. Schlenoff, J. B., Zwitteration: coating surfaces with zwitterionic functionality to reduce nonspecific adsorption. *Langmuir* **2014,** *30* (32), 9625-9636.
24. Chen, S.; Zheng, J.; Li, L.; Jiang, S., Strong resistance of phosphorylcholine self-assembled monolayers to protein adsorption: insights into nonfouling properties of zwitterionic materials. *Journal of the American Chemical Society* **2005,** *127* (41), 14473-14478.
25. Holmlin, R. E.; Chen, X.; Chapman, R. G.; Takayama, S.; Whitesides, G. M., Zwitterionic SAMs that resist nonspecific adsorption of protein from aqueous buffer. *Langmuir* **2001,** *17* (9), 2841-2850.
26. Jiang, S.; Cao, Z., Ultralow-fouling, functionalizable, and hydrolyzable zwitterionic materials and their derivatives for biological applications. *Advanced Materials* **2010,** *22* (9), 920-932.
27. Vaisocherová, H.; Zhang, Z.; Yang, W.; Cao, Z.; Cheng, G.; Taylor, A. D.; Piliarik, M.; Homola, J.; Jiang, S., Functionalizable surface platform with reduced nonspecific protein adsorption from full blood plasma—Material selection and protein immobilization optimization. *Biosensors and Bioelectronics* **2009,** *24* (7), 1924-1930.
28. Wang, T.; Kou, R.; Liu, H. L.; Liu, L. D.; Zhang, G. Z.; Liu, G. M., Anion specificity of polyzwitterionic brushes with different carbon spacer lengths and its application for controlling protein adsorption. *Langmuir* **2016,** *32* (11), 2698-2707.
29. Wang, T.; Wang, X. W.; Long, Y. C.; Liu, G. M.; Zhang, G. Z., Ion-specific conformational behavior of polyzwitterionic brushes: exploiting it for protein adsorption/desorption control. *Langmuir* **2013,** *29* (22), 6588-6596.

30. Piliarik, M.; Homola, J., Self-referencing SPR imaging for most demanding high-throughput screening applications. *Sens. Actuator B-Chem.* **2008,** *134* (2), 353-355.
31. Piliarik, M.; Bockova, M.; Homola, J., Surface plasmon resonance biosensor for parallelized detection of protein biomarkers in diluted blood plasma. *Biosens. Bioelectron.* **2010,** *26* (4), 1656-1661.
32. Homola, J., Surface plasmon resonance sensors for detection of chemical and biological species. *Chemical Reviews* **2008,** *108* (2), 462-493.
33. Luo, S. R.; Yau, S. L.; Kumaresan, P.; Vegiraju, S.; Chen, M.-C., Scanning tunneling microscopy examination of rubrene deposited on Au(111) in aqueous solution. *The Journal of Physical Chemistry C* **2015,** *119* (3), 1376-1381.
34. Liu, C. Y.; Huang, C. J., Functionalization of polydopamine via the aza-Michael reaction for antimicrobial interfaces. *Langmuir* **2016,** *32* (19), 5019-5028.
35. Huang, C. J.; Wang, L. C., Bio-inspired multifunctional catecholic assembly for photo-programmable biointerface. *Colloid Surf. B-Biointerfaces* **2015,** *134*, 247-253.
36. Castner, D. G.; Hinds, K.; Grainger, D. W., X-ray photoelectron spectroscopy sulfur 2p study of organic thiol and disulfide binding interactions with gold surfaces. *Langmuir* **1996,** *12* (21), 5083-5086.
37. Yang, W. J.; Neoh, K.-G.; Kang, E.-T.; Lay-Ming Teo, S.; Rittschof, D., Stainless steel surfaces with thiol-terminated hyperbranched polymers for functionalization via thiol-based chemistry. *Polymer Chemistry* **2013,** *4* (10), 3105-3115.
38. Huang, C. J.; Wang, L. C.; Shyue, J. J.; Chang, Y. C., Developing antifouling biointerfaces based on bioinspired zwitterionic dopamine through pH-modulated assembly. *Langmuir* **2014,** *30* (42), 12638-12646.
39. Wu, C. J.; Huang, C. J.; Jiang, S. Y.; Sheng, Y. J.; Tsao, H. K., Superhydrophilicity and spontaneous spreading on zwitterionic surfaces: carboxybetaine and sulfobetaine. *RSC Adv.* **2016,** *6* (30), 24827-24834.
40. Weers, J. G.; Rathman, J. F.; Axe, F. U.; Crichlow, C. A.; Foland, L. D.; Scheuing, D. R.; Wiersema, R. J.; Zielske, A. G., Effect of the intramolecular charge separation distance on the solution properties of betaines and sulfobetaines. *Langmuir* **1991,** *7* (5), 854-867.
41. Laughlin, R. G., Fundamentals of the zwitterionic hydrophilic group. *Langmuir* **1991,** *7* (5), 842-847.
42. Zhang, Z.; Vaisocherová, H.; Cheng, G.; Yang, W.; Xue, H.; Jiang, S., Nonfouling behavior of polycarboxybetaine-grafted surfaces: structural and environmental effects. *Biomacromolecules* **2008,** *9* (10), 2686-2692.
43. Georgiev, G. S.; Karnenska, E. B.; Vassileva, E. D.; Kamenova, I. P.; Georgieva, V. T.; Iliev, S. B.; Ivanov, I. A., Self-assembly, anti polyelectrolyte effect, and nonbiofouling properties of polyzwitterions. *Biomacromolecules* **2006,** *7* (4), 1329-1334.
44. Izumrudov, V. A.; Domashenko, N. I.; Zhiryakova, M. V.; Davydova, O. V., Interpolyelectrolyte reactions in solutions of polycarboxybetaines, 2: Influence of alkyl spacer in the betaine moieties on complexing with polyanions. *J. Phys. Chem. B* **2005,** *109* (37), 17391-17399.
45. Vericat, C.; Vela, M. E.; Benitez, G.; Carro, P.; Salvarezza, R. C., Self-assembled monolayers of thiols and dithiols on gold: new challenges for a well-known system. *Chem. Soc. Rev.* **2010,** *39* (5), 1805-1834.

46. Leopold, M. C.; Bowden, E. F., Influence of gold substrate topography on the voltammetry of cytochrome c adsorbed on carboxylic acid terminated self-assembled monolayers. *Langmuir* **2002,** *18* (6), 2239-2245.
47. Creager, S. E.; Clarke, J., Contact-angle titrations of mixed omega-mercaptoalkanoic acid alkanethiol monolayers on gold-reactive vs nonreactive spreading, and chain-length effects on surface pK(a) values. *Langmuir* **1994,** *10* (10), 3675-3683.
48. Smith, C. P.; White, H. S., Voltammetry of molecular films containing acid-base groups. *Langmuir* **1993,** *9* (1), 1-3.
49. Ding, S.-J.; Chang, B.-W.; Wu, C.-C.; Lai, M.-F.; Chang, H.-C., Impedance spectral studies of self-assembly of alkanethiols with different chain lengths using different immobilization strategies on Au electrodes. *Analytica Chimica Acta* **2005,** *554* (1), 43-51.
50. Zhou, C.; Khlestkin, V. K.; Braeken, D.; De Keersmaecker, K.; Laureyn, W.; Engelborghs, Y.; Borghs, G., Solvent-controlled organization of self-assembled polymeric monolayers on gold: an easy approach for the construction of protein resistant surfaces. *Langmuir* **2005,** *21* (13), 5988-5996.
51. Cannes, C.; Kanoufi, F.; Bard, A. J., Cyclic voltammetric and scanning electrochemical microscopic study of menadione permeability through a self-assembled monolayer on a gold electrode. *Langmuir* **2002,** *18* (21), 8134-8141.
52. Shen, C.-H.; Lin, J.-C., Solvent and concentration effects on the surface characteristics and platelet compatibility of zwitterionic sulfobetaine-terminated self-assembled monolayers. *Colloids and Surfaces B: Biointerfaces* **2013,** *101* (Supplement C), 376-383.
53. Huang, C. J.; Lin, Z. E.; Yang, Y. S.; Chan, H. W. H.; Chen, W. Y., Neutralized chimeric DNA probe for detection of single nucleotide polymorphism on surface plasmon resonance biosensor. *Biosens. Bioelectron.* **2018,** *99*, 170-175.
54. Tsai, W. B.; Grunkemeier, J. M.; Horbett, T. A., Human plasma fibrinogen adsorption and platelet adhesion to polystyrene. *J. Biomed. Mater. Res.* **1999,** *44* (2), 130-139.
55. Devi, J. M., Molecular simulations of mixed self-assembled monolayer coated gold nanoparticles in water. *J. Mol. Model.* **2015,** *21* (6).
56. Pollet, J.; Delport, F.; Janssen, K. P. F.; Tran, D. T.; Wouters, J.; Verbiest, T.; Lammertyn, J., Fast and accurate peanut allergen detection with nanobead enhanced optical fiber SPR biosensor. *Talanta* **2011,** *83* (5), 1436-1441.

TOC: